OPTIMIZE INJECTION MOLDING CYCLES FOR HDPE BY CONSIDERING THE EFFECT OF COOLING TIMES ON PART PEFORMANCE

C.M. Dickerson, Equistar Chemicals, LP

W.G. Todd, Ph.D., Equistar Chemicals, LP

T.J. Schwab, Equistar Chemicals, LP

D.L. Wise, Equistar Chemicals, LP

ABSTRACT

Many different grades of high density polyethylene (HDPE) are used in the production of injection molded rigid containers that are widely used in food packaging and promotional drink cups.[1] These grades are differentiated from each other by their physical properties, such as molecular weight, molecular weight distribution, density, comonomer type and antioxidant level. Material physical properties and processing conditions often dictate end-use part performance. This paper investigates the relationship between injection molding cycle time manipulation via cooling time selection and the part performance of two grades of HDPE.

INTRODUCTION

From previous work[1,2], it was discussed how to relate the processability and end-use physical properties for high-flow HDPE products back to the manufacturing synthesis conditions and resin physical properties. These models provide improved resin design and result in optimized physical properties.

Resin conversion processing conditions also contribute to the end-use properties exhibited by parts molded from HDPE. Molders of thin-walled rigid food packaging and drink cups have an interest in reducing production cycle times in order to improve process efficiency. This task can often be achieved by reducing time allocations provided to the clamping segment of injection molding machines. Reducing cooling times and mold open times can often achieve the most effective cycle time reductions. While some material grades lend themselves

more effectively to cycle time reductions than others, careful attention must always be paid to the variation in part performance as a function of the cycle time.

DISCUSSION

Molders of thin-walled rigid packaging and drink cups are posed with the challenging task of producing quality parts in a timely, efficient manner. They require a resin that can be easily processed into molds with demanding aspect ratios, yet will maintain the desired physical properties after being converted into end-use parts.

Resin converters continually look for process improvements that lead to decreased cycle times and hence more efficient manufacturing practices. Improvements in resin design can aid resin converters in the pursuit of more efficient manufacturing processes; however, the effects of cycle time variation on end-use part performance must be understood.

Fast injection speeds and complete mold filling for thin-walled rigid food packaging and drink cups, require a resin with excellent flow characteristics. Traditionally the processability of a resin is measured using Melt Index (MI_2). MI_2 is typically used as an estimate of molecular weight by measuring the number of grams of polymer extruded in 10 minutes, as tested by ASTM D 1248. Generally as the melt index increases, the molecular weight decreases, thus improving the processability of the resin. Some resin manufacturers can also improve the processability of the resin by manipulating the resin to a broader molecular weight distribution (MWD). To estimate the MWD of a HDPE product the melt flow ratio (MFR) is typically used. This calculated number is the ratio of a melt index measured at high shear rates (MI_{20}) to a melt index measured at low shear rates (MI_2). At a given MI a broader MWD normally has improved processing properties; however, the improved processing typically comes with the undesired trade-off of decreased impact resistance.

The cooling and mold open times can be critical bottlenecks in the molding process. A resin producer can help facilitate a reduction in these times by producing a resin that can be ejected from the mold at elevated temperatures. This can be accomplished by producing a stiffer resin. One measure of the stiffness of a resin is the flexural modulus, as determined by ASTM D 790. A higher flexural modulus corresponds to a stiffer material. An increase in the flexural modulus can typically be achieved by increasing the density, as determined

by ASTM D 1505, of the product. Density measures the crystallinity of the resin and is a function of the amount of comonomer incorporated into the resin. A decrease in comonomer incorporation will increase the density of HDPE. An increase in density and hence crystallinity, also provides a cooling cycle advantage by effectively increasing the crystallization temperature of the material. This means that less sensible heat must be removed in order to begin the crystallization process; therefore, less time is needed to obtain a solid part. One disadvantage of increasing the density is typically a decrease in the impact resistance of the end-use parts.

Resin converters must analyze the effects of the cycle time manipulation on the end-use part properties. Important end-use part properties for the thin-walled rigid food packaging and drink cup markets include topload strength, lip-integrity/tensile strength and impact resistance.

EXPERIMENTAL

The physical properties of the two resins used in this study are listed in Table 1. Both resins are commercially available high-flow HDPE products. As is shown with their similar spiral flow numbers and based on previous work[1], these products have similar high shear viscosities and will process comparably to each other during injection molding. The spiral flow number is a comparative measure used to analyze the flow characteristics of a resin under actual injection molding conditions. It is determined by measuring the length in centimeters of flow when molten resin at 227ºC is injection molded into a long spiral-channel insert (half-round 0.635 x 0.157 cm x 127 cm) at a constant pressure of 6.9 MPa.

For this study 83- ounce containers were molded on a 330-Ton Husky injection molding machine. The cooling times were varied for each material while the extruder temperatures, injection profile, hold profile and recovery profile remained constant due to the similar viscosities of each resin. Parts were tested for lip integrity, topload strength and drop impact. **Lip integrity** provides a measure of tensile strength of the part. The lip integrity test was conducted on an Instron® at a crosshead speed of 1.25 cm/min. The bottom of the container was attached to the base of the Instron while the lip of the container was connected to a gripping fixture and pulled until a failure was recorded. **Topload strength** provides a measure of part rigidity. The topload strength test was conducted on an Instron at a crosshead speed of 2.5 cm/min. The maximum load on the container before failure was measured. **Drop impact** provides a measure of part impact resistance. The drop impact test was conducted at 4.4ºC by filling

the containers with water. The F_{50} value for this test was determined by flat bottom dropping the containers from various heights. Results from the part testing are shown in Tables 2 – 4.

To aid in the analysis of the data within a sample set, molded parts from the various cooling times were microtomed and analyzed via optical microscopy. Using an Olympus BX50 microscope/Sony CCD IRIS video camera with Image Pro Plus 4.0 software, photomicrographs of the gate, chime, and lip cross-sections were taken. Previous work has shown that microscopy of **microtomed** samples provides a visual representation of the flow patterns and crystalline boundary regions within a cross-sectional sample. The crystalline boundary regions typically consist of amorphous skin layers and inner crystalline layers, each containing discrete crystalline morphology based on the material heat history and cooling characteristics. The crystalline boundaries play an important role in determining the physical properties of the end-use part. Polarized light was used in order to aid in the identification of crystalline boundaries and molded-in stresses.

DATA ANALYSIS

Part cooling times were varied between 1.1 s and 8 s for each material. Note that there is no data displayed for resin A at the cooling time of 1.1 s. Resin A did not possess the required stiffness needed in order to be ejected from the mold at a cooling time of 1.1 s. This is an expected result that one can infer from the density listing in Table 1. Resin B is higher in density and is therefore expected to maintain a higher stiffness than resin A, thus providing easier part ejection at elevated temperatures.

Topload Strength

Table 2 provides topload strength data for the two resins evaluated in this study. For all cooling times, resin B maintains top-load strength superiority over resin A. This is an expected result, as Resin B inherently possesses a greater degree of crystallinity than resin A and is predicted to exhibit a greater stiffness. Figure 1 and Figure 2 are photomicrographs of sidewall cross sections of the parts molded from resin A and resin B at a cooling time of 2 seconds. The thicker inner crystalline layer and higher density displayed by B, aid in providing the greater topload strength properties exhibited by resin B. Variations in cooling times did little to affect a change in topload strength properties.

Lip Pull Integrity

Table 3 provides lip pull integrity data for the two resins evaluated in this study. In both cases, lip pull integrity increases with increasing cooling times. Resin A and resin B possess similar lip pull integrity characteristics below three seconds of cooling time. At or above 3 seconds of cooling time resin B exhibits better lip pull integrity when compared to resin A. A trend of increasing lip pull integrity with increasing cooling times is likely seen due to an increase in the amorphous skin layer thickness as cooling times increase. The amorphous skin layer provides additional lip elongation characteristics and crack resistance, which allows for greater lip deflection before failure is incurred. The ability of the lip to deflect without cracking and the rigidity of the inner crystalline layer both combine to provide the observed lip pull integrity. Resin B obtained the best balance of these properties at 8 seconds of cooling time as can be seen in table 3.

Drop Impact Resistance

Table 4 provides drop impact resistance data for the two resins evaluated in this study. Both resins initially exhibit increased impact resistance with increasing cooling times. Both materials reach a maximum impact resistance at around three to four seconds of cooling time. Beyond three to four seconds of cooling

2290/0715

time, the impact resistance for both materials begins to decline. Resin A displays superior impact resistance properties in comparison to resin B for all cooling times, which is primarily the result of having a lower density. The impact properties also follow the thickness of the amorphous skin layers of the parts. The amorphous skin layers are lower in crystallinity than the inner layer and provide impact resistance properties for the part. Figure 3 and figure 4 are photomicrographs of gate cross sections of the parts molded from resin A and resin B at a cooling time of 4 seconds. Resin A consistently displays thicker amorphous skin layers than resin B for all cooling times and therefore exhibits superior impact resistance properties than resin B. This is expected as resin B is inherently higher in crystallinity than resin A. Both materials exhibit a maximum amorphous skin layer thickness at three to four seconds of cooling time.

SUMMARY

Some resin manufacturers are capable of tailoring resins to meet the needs of their customers by balancing resin processing, impact resistance and stiffness properties. Resin B is an example of a resin engineered for the thin-walled packaging and drink cup markets. It possesses superior stiffness, which aids part ejection at short cooling cycles.

Resin converters who modify cycle times by manipulating mold cooling times must acknowledge and understand the changes in end-use part performance affected by those modifications. If resin converters wish to maximize the balance of physical properties displayed by the end-use parts, the cooling time and hence the cycle time must be optimized.

ACKNOWLEDGEMENTS

REFERENCES

[1] Todd, W. G., Wise, D. L. & Williams, H.: Plastics-Bridging the Millennia, ANTEC 1999 Proceedings
[2] Todd, W.G., Schwab, T.J., & Wise, D.L.: ANTEC 2000 Proceedings.

Table 1: Experimental Resin and Results

Resin	Melt Index	Density	MFR	Spiral Flow Number	Flexural Modulus (1% Secant)*	Unnotched Izod at 18°C*	Peak Melting Temp	Peak Crystallization Temp
	(g/10 min.)	(g/cc)		(cm)	(MPa)	(J/m)	(°C)	(°C)
A	56.5	0.947	31.0	53.3	896	261	126	112
B	55.5	0.956	30.3	52.3	1110	192	129	116

*Tested using injection molded ASTM type I compression molded parts

Table 2: Top Load Strength 83 oz. Containers (N)
Cooling Time (s)

Material	1.1	1.5	2	3	4	5	6	8
A	NA	696	696	683	681	692	701	695
B	943	941	944	938	920	925	925	914

Figure 1: Resin A Cross-Section of Part Sdewall. Two Seconds Cooling Time, 4X Magnification
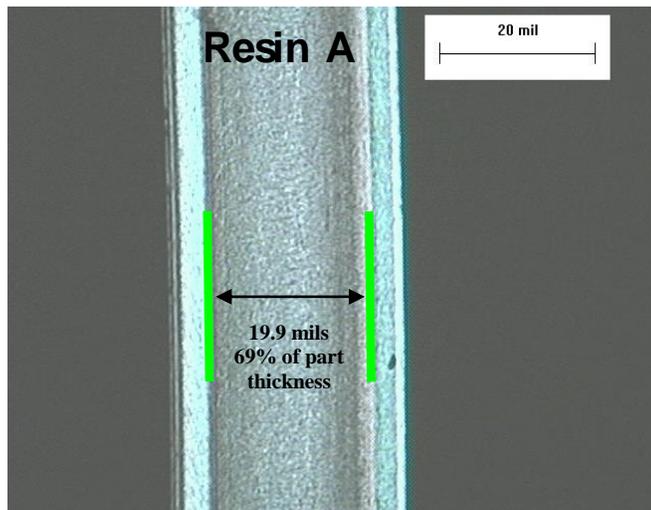
Figure 2: Resin B Cross-Section of Part Sdewall. Two Seconds Cooling Time, 4X Magnification
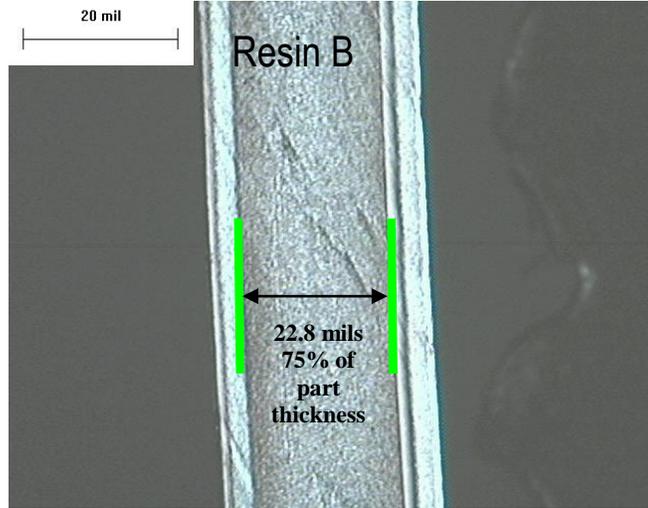
Table 3: Lip Pull Strength 83 oz. Containers (N)

Cooling Time (s)

Material	1.1	1.5	2	3	4	5	6	8
A	NA	898	978	1,117	1,206	1,266	1,253	1,283
B	730	868	917	1,115	1,239	1,316	1,417	1,412

Table 4: F-50 Heights (m)-40°F Water in 83 oz. Containers

Cooling Time (s)

Material	1.1	1.5	2	3	4	5	6	8
A	NA	2.38	2.44	3.79	3.63	3.25	3.10	2.47
B	1.35	1.73	1.41	2.16	2.95	2.64	1.73	1.50

Figure 3: Resin A Cross-Section of Part Gate. Four Seconds Cooling Time, 4X Magnification

Core side, 9.2 mils

Cavity side, 7.4 mils
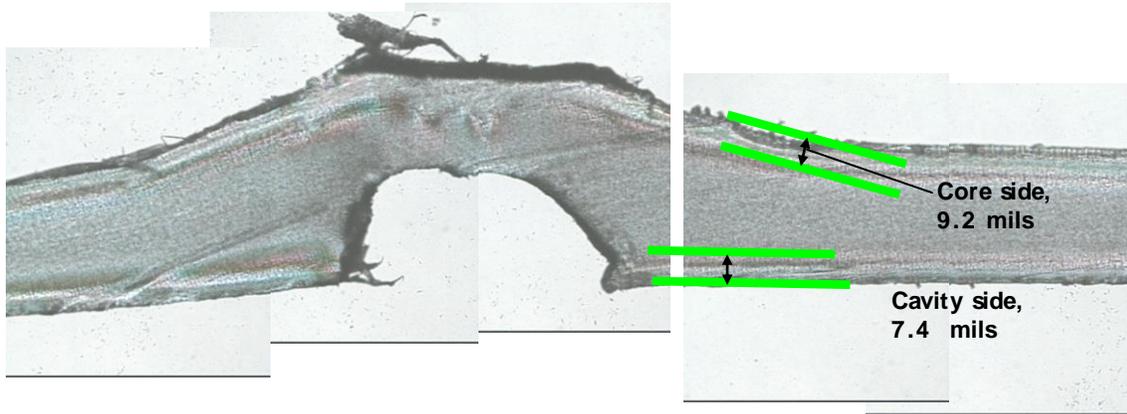
Figure 4: Resin B Cross-Section of Part Gate. Four Seconds Cooling Time, 4X Magnification

Core side, 8.1 mils

Cavity Side, 6.7 mils
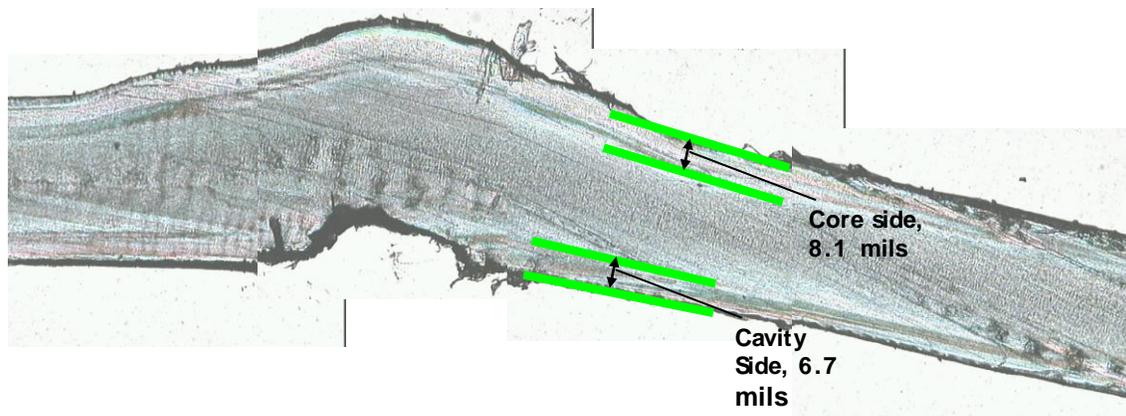
lyondellbasell

LyondellBasell Industries
P.O. Box 3646
Houston, TX 77252-3646
United States

www.LYB.com